




Article

Modeling Thermal Effects of Pulsating Currents in Human Tissues: How to Prevent Necrosis

Angiolo Farina ^{1,*} , Antonio Fasano ^{1,2,†}  and Fabio Rosso ^{1,†} 

¹ Dipartimento di Matematica e Informatica “Ulisse Dini”, Università degli Studi di Firenze, Viale Morgagni, 67/a, 50134 Firenze, Italy; a.fasano@fiab.it (A.F.); fabio.rosso@unifi.it (F.R.)

² FIAB SpA, Vicchio, 50039 Firenze, Italy

* Correspondence: angiolo.farina@unifi.it

† These authors contributed equally to this work.

Abstract: In certain clinical applications, pulsating currents are applied to specific body regions for therapeutic purposes. In this paper, we analyze the resulting thermal field to determine the optimal amplitude, period, and duration of these stimuli, ensuring that the temperature in the targeted tissue remains below the necrosis threshold.

Keywords: electric pulses; blood perfusion; safe operational ranges

1. Introduction

Transesophageal cardiac pacing (TECP) is a well-established medical practice (see, e.g., [1]) that has long been considered safe. In fact, it is currently employed in procedures for immature newborns as well [2]. The procedure involves delivering periodic voltage pulses to the patient’s atrium, using a bipolar stimulator placed in the esophagus.

However, a case study reported in [3] raised concerns by documenting a serious esophageal lesion after prolonged transesophageal pacing, though the specific device used was not mentioned. The report cautioned that extended current delivery in a localized area may pose risks. This is particularly important, considering the growing experience in cardiac radio frequency ablation for atrial fibrillation, which has demonstrated that even a modest temperature increase (as little as 3–4 °C above baseline) can cause esophageal damage (a thorough review is available in [4]).

The literature extensively documents the harmful effects of mild hyperthermia on biological tissues. For instance, Pearce’s work [5] and the review found in [6] (Chapter 7) confirm that tissue reactions to heat can vary significantly from patient to patient, though the damage threshold is generally consistent.

The incident reported in [3] has not yet been fully explained, motivating us to investigate the phenomenon further. Our goal is to analyze the temperature increase caused by the application of periodic voltage pulses, ranging from 1 to 20 V, applied between electrodes positioned at a short distance from each other within a body cavity. This analysis will allow us to define a safety range for such procedures, preventing thermal necrosis.

One physiological factor that plays a crucial role in this context is local acidity, as it strongly influences electrical conductivity. We hypothesize that the adverse event described in [3] was most likely caused by gastric reflux. In this paper, we calculate the steady-state thermal field created by a periodic current, with a focus on the influence of the physical parameters that are most relevant to this procedure. Furthermore, we determine the safety limits that should be observed.

In our initial calculations, we will exclude the effects of tissue blood perfusion, and then assess how much perfusion contributes to dissipating the heat. We also highlight that the methodology we propose could be adapted for other similar medical procedures, such as pulsed field ablation (PFA). PFA has recently been introduced for isolating pulmonary veins



Citation: Farina, A.; Fasano, A.; Rosso, F. Modeling Thermal Effects of Pulsating Currents in Human Tissues: How to Prevent Necrosis. *Biophysica* **2024**, *4*, 477–487. <https://doi.org/10.3390/biophysica4040031>

Academic Editor: Morten Gram Pedersen

Received: 18 August 2024

Revised: 23 September 2024

Accepted: 26 September 2024

Published: 27 September 2024



Copyright: © 2024 by the authors. Licensee MDPI, Basel, Switzerland. This article is an open access article distributed under the terms and conditions of the Creative Commons Attribution (CC BY) license (<https://creativecommons.org/licenses/by/4.0/>).

in the treatment of atrial fibrillation (see, e.g., [7]). This procedure employs highly intense electric fields that cause irreversible electroporation of targeted cells, and necessitates additional analysis of heat dissipation due to the strong blood flow from the left atrium to the ventricle. As such, the geometric model we use in this paper may not be fully suitable for the PFA case, which will be addressed in a future study.

2. The Physical Setting and a First, Approach

We consider the case in which the electrodes are introduced in a body cavity, generating a pulsating electric field for therapeutic purposes. Of course, the electric field extends over the whole body, but it rapidly diminishes with distance from the source. A first simplifying assumption we make is to suppose that heat is generated by a uniform pulsating current confined in a spherical region of radius R around the electrodes. The current has a duration t_s and a period $t_b > t_s$, see Figure 1. In our approach, the power delivered is considered constant, i.e., averaged over a period, considering that $t_b (< 2 \text{ s})$ is much shorter than the application time t_{ref} (typically in the order of hours).

We further assume that heat diffuses outward from this spherical region into a larger sphere with radius R_e (for instance $R_e = 10 R$; typically $R = 5 \text{ mm}$, $R_e = 5 \text{ cm}$, as illustrated in Figure 2). The boundary of this larger sphere is maintained at a constant temperature T_0 , representing the patient's basal temperature. In this model, we neglect any potential thermal inhomogeneities within the tissue, which is reasonable given the level of approximation we are targeting.

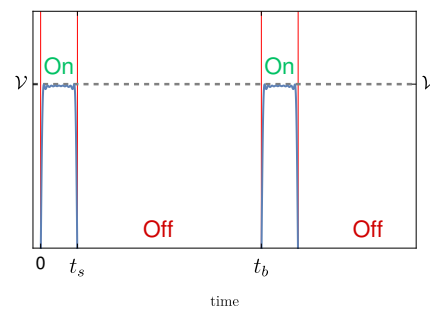


Figure 1. Delivered voltage versus time for a given voltage \mathcal{V} and a given duty cycle t_s/t_b (ratio of the pulse duration over the time it takes the signal to complete an on-off cycle).

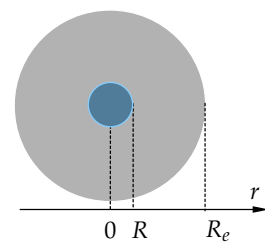


Figure 2. Area of action of the apparatus (the two radii are not in scale, for visualization purposes).

The choice of the radius R_e is not critical. It just represents a distance at which the influence of the temperature variation taking place in the sphere of radius R becomes ineffective. What really matters is that the ratio $\varepsilon = R/R_e$ is much smaller than unity. In the following, we will simply let R_e go to infinity. The resulting expression of the thermal field will be approximated at the first order in ε . One more simplification can be achieved considering the time scale involved. As we said, the procedure time, which is our reference time t_{ref} , is in the order of hours. This has to be compared with the diffusion time t_d , defined (see [8]) as the time heat takes to substantially affect the medium at a distance of the order R , namely $R^2 \rho c / k$, where ρ is density, c is specific heat, and k is thermal conductivity. Typical values for living tissues are $\rho = 10^3 \text{ kg m}^{-3}$, $c = 3.5 \times 10^3 \text{ J kg}^{-1} \text{ K}^{-1}$, $k = 0.5 \text{ W m}^{-1} \text{ K}^{-1}$, implying $t_d \approx 175 \text{ s}$. Hence, $t_d/t_{\text{ref}} \ll 1$. This circumstance indicates that we are just

interested to the asymptotic thermal field, thus dropping time dependence. For the time being, in order to concentrate on the main aspects of the model, we neglect the effects of blood perfusion, which will be introduced later. Thus, the equation to be satisfied by the temperature T is simply the one of the steady state

$$-k \left(\frac{\partial^2 T}{\partial r^2} + \frac{2}{r} \frac{\partial T}{\partial r} \right) = P(r), \quad (1)$$

where $P(\bar{r})$ denotes the time averaged power delivery rate per unit volume, namely

$$P(r) = \begin{cases} \frac{3Q}{4\pi R^3}, & \text{if } 0 < r < R, \\ 0, & \text{if } R < r < R_e, \end{cases} \quad (2)$$

with Q being the average power delivered into the sphere because of Joule effect. When the stimulation is on, the power supplied is $\mathcal{V}^2 / \mathcal{Z}$, where \mathcal{V} is the stimulation amplitude and \mathcal{Z} is the medium impedance; therefore,

$$Q = \frac{t_s}{t_b} \mathcal{V}^2 / \mathcal{Z}, \quad (3)$$

where, as we said, t_b is the pulse period and $t_s (< t_b)$ is the current delivery time. It is now convenient to adopt the dimensionless radius r/R , for which we still use the symbol r . Moreover, instead of T , we consider the difference $\vartheta = T - T_o$, where T_o is the patient's basal temperature (≈ 310 K). Doing so, the governing differential equation becomes

$$- \left(\frac{\partial^2 \vartheta}{\partial r^2} + \frac{2}{r} \frac{\partial \vartheta}{\partial r} \right) = \frac{1}{k} \frac{3Q}{4\pi R} \mathcal{H}[1 - r], \quad (4)$$

where $\mathcal{H}(1 - r) = 1$ for $0 < r < 1$ and zero otherwise. We also define

$$\mathfrak{F}(r) = \frac{1}{k} \frac{3Q}{4\pi R} \mathcal{H}[1 - r], \quad (r > 0), \quad (5)$$

measured in Kelvin degrees. Equation (4) is supplemented by the boundary conditions $\partial \vartheta / \partial r = 0$ for $r = 0$ (no flow through the center) and $\vartheta = 0$ at infinity. Moreover, heat flux and temperature must be continuous across the interface $r = 1$ (i.e., at R). Now, we shift our attention to the impedance \mathcal{Z} .

We may write $\mathcal{Z} = 1/(\sigma L)$, where σ is the medium electrical conductivity (measured in Sm^{-1} , $S = \text{Siemens}$), and L can be taken as the side of a cubic box whose volume is equal to that of the sphere of radius R , i. e. $L = (4\pi/3)^{1/3} R$. Consequently, recalling (3), we can rewrite (5) as

$$\mathfrak{F}(r) = G \mathcal{V}^2 \frac{\sigma t_s}{k t_b} \mathcal{H}[1 - r], \quad (r > 0) \quad (6)$$

where

$$G = (3/4\pi)^{2/3} \approx 0.385. \quad (7)$$

The expression (6) of the source term emphasizes the role of the three parameters \mathcal{V} , t_s , t_b , settable by the operator and of the physical properties of the medium entering as the ratio σ/k , thus indicating that the two conductivities act in opposite ways.

Though the radius R has eventually disappeared from our main estimates, it is interesting to check whether our guess ($R = 5$ mm) was sensible. People working in the area of electrostimulation (see, e.g., [9]) normally take the empirical assumption that the resistive load offered to the generator is 300–500 Ω . So far, we did not make any use of this information because it is too generic, but it can give a reasonable idea of the size of R , using $R = (3/4\pi)^{1/3} (\sigma \mathcal{Z})^{-1}$. Setting $\sigma = 0.4 \text{ Sm}^{-1}$ (as we shall see for the normal environment),

and choosing \mathcal{Z} in the above interval, we obtain R between ≈ 3 and 5 mm, in accordance with our guess.

Taking into account the boundary and interface conditions for ϑ , the differential system to be solved for ϑ is

$$\begin{cases} \vartheta'' + \frac{2}{r}\vartheta' = -\mathfrak{F}(r), & r > 0 \\ \lim_{r \rightarrow +\infty} \vartheta(r) = 1, & \vartheta'(0) = 0 \\ \llbracket \vartheta \rrbracket|_{r=1} = \llbracket \vartheta' \rrbracket|_{r=1} = 0. \end{cases} \tag{8}$$

It can be easily checked that the solution is written as

$$\vartheta(r) = \begin{cases} \frac{G}{2} \left(\mathcal{V}^2 \frac{\sigma}{k} \frac{t_s}{t_b} \right) \left(1 - \frac{r^2}{3} \right), & 0 < r < 1 \\ \frac{G}{3} \left(\mathcal{V}^2 \frac{\sigma}{k} \frac{t_s}{t_b} \right) \frac{1}{r}, & r \geq 1 \end{cases} \tag{9}$$

Notice that function ϑ is always ≥ 0 , and takes its maximum as $r = 0$. Using \mathcal{H} , we can rewrite (9) as

$$\vartheta(r) = \frac{G}{2} \left(\mathcal{V}^2 \frac{\sigma}{k} \frac{t_s}{t_b} \right) \left[\left(1 - \frac{r^2}{3} \right) \mathcal{H}[1 - r] + \frac{2}{3r} \mathcal{H}[r - 1] \right]. \tag{10}$$

Figures 3 and 4 show how ϑ changes by changing the operational parameters, considering a reasonable range for σ (generally 0.4 but exceptionally up to 2 Sm⁻¹ or more), $k = 0.5 \text{ Wm}^{-1} \text{ K}^{-1}$, and the usual instrument operational intervals ($\mathcal{V} \in (0.5, 20) \text{ V}$, $t_s \in (1, 20) \text{ ms}$, and $t_b \in (50, 2000) \text{ ms}$).

Working with the temperature at the center may, however, be too heavy a condition, since the sphere of (dimensionless) radius $r = 1$ is more likely occupied by a liquid medium, namely the cellular tissue being more or less at the boundary of the ideal sphere in which we have confined the current. Therefore, a more interesting temperature seems to be the one calculated at $r = 1$ (see Figures 3 and 4), namely from (9),

$$\vartheta(1) \approx \frac{G}{3} \mathcal{V}^2 \frac{t_s}{t_b} \frac{\sigma}{k}. \tag{11}$$

It is reasonable to suppose that (11) provides the maximal temperature difference to which the tissue is exposed. Our goal now is to investigate the safety condition $\vartheta(1) \leq \delta$, where δ is a suitable threshold. A conservative value for δ could be 3 K.

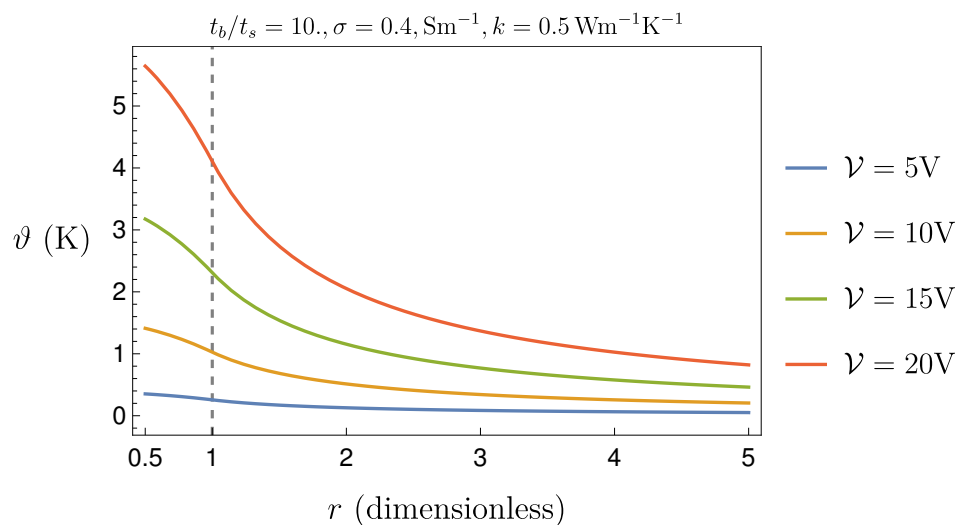


Figure 3. Function $\vartheta(r)$ for $t_b/t_s = 10$, $\sigma = 0.4 \text{ Sm}^{-1}$, $k = 0.5 \text{ Wm}^{-1} \text{ K}^{-1}$, and varying \mathcal{V} between 0.5 V and 20 V. The clinically interesting region occurs for $r > 1$.

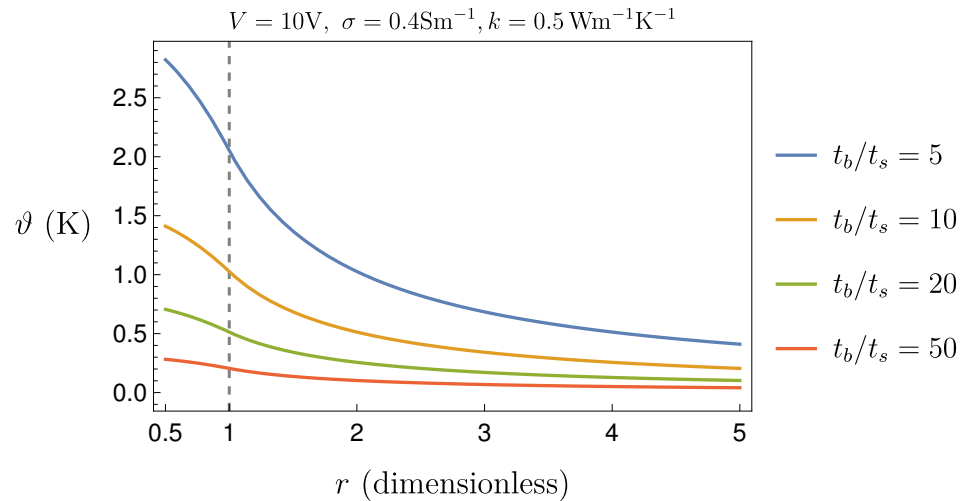


Figure 4. Function $\vartheta(r)$ for $\mathcal{V} = 10\text{ V}$, $\sigma = 0.4\text{ Sm}^{-1}$, $k = 0.5\text{ Wm}^{-1}\text{ K}^{-1}$, and varying t_b/t_s between 5 and 50. The clinically interesting region occurs for $r > 1$.

3. Safety Stimulating Conditions

Let us define

$$\mathcal{A}(\mathcal{V}, t_s, t_b, \sigma, k) = \delta - \frac{G}{3} \mathcal{V}^2 \frac{t_s \sigma}{t_b k}, \quad (12)$$

so that the safety condition becomes

$$\mathcal{A}(\mathcal{V}, t_s, t_b, \sigma, k) > 0. \quad (13)$$

While the thermal conductivity k for biological tissues is more or less constant with typical value $0.5\text{ Wm}^{-1}\text{ K}^{-1}$ (with the exception of fat; see, e.g., [10]), the electrical conductivity σ is strongly affected by the pH of the ambient. We may first assume that the conductive medium filling the sphere of radius R is aqueous (e.g., saliva, as it happens in the esophagus). In that case, ref. [11] provides for σ values between 3.5 m Scm^{-1} and 4.7 m Scm^{-1} . Passing to SI units ($1\text{ m Scm}^{-1} = 0.1\text{ Sm}^{-1}$), we take a typical value $\sigma = 0.4\text{ Sm}^{-1}$. Thus, for $\delta = 3\text{ K}$, the safety condition (13) is to be read as

$$\mathcal{V}^2 \frac{t_s}{t_b} < \frac{3\delta k}{G \sigma} \text{V}^2 \approx 29 \text{V}^2. \quad (14)$$

This result has to be examined in view of the range of the parameters \mathcal{V} , t_s , t_b practically available on the devices employed.

If we set $x = t_b/t_s$, then condition (14) entails, approximately,

$$\mathcal{V} < 5.4\sqrt{x} \text{V}, \quad (15)$$

where $x \in (2.5, 2000)$.

The interval of positiveness of the function $\mathcal{A}(\mathcal{V}, x, 0.4, 0.5)$ identifies the safety ratio $x = t_b/t_s$ for any given \mathcal{V} or, vice versa, the safe voltage \mathcal{V} for any given ratio t_b/t_s . Figures 5 and 6 show, respectively, the cases $\mathcal{V} = 20\text{ V}$ and $x = 2.5$.

This result indicates that the procedure is feasible, even with the largest stimulation amplitude ($\mathcal{V} = 20\text{ V}$), but with a suitable control of the ratio t_b/t_s (for instance, if $t_b = 1\text{ s}$, then $t_s < 70\text{ ms}$ would be fine). According to (11), the adoption of the extreme values settable on the generator ($\mathcal{V} = 20\text{ V}$ and $x = 2.5$) gives a maximal temperature increase of about 16 K , which is far beyond criticality. Therefore, it is not suggestible to set the generator parameters at their extreme values, though it would be sufficient, e.g., to keep the pulse duration t_s sufficiently low.

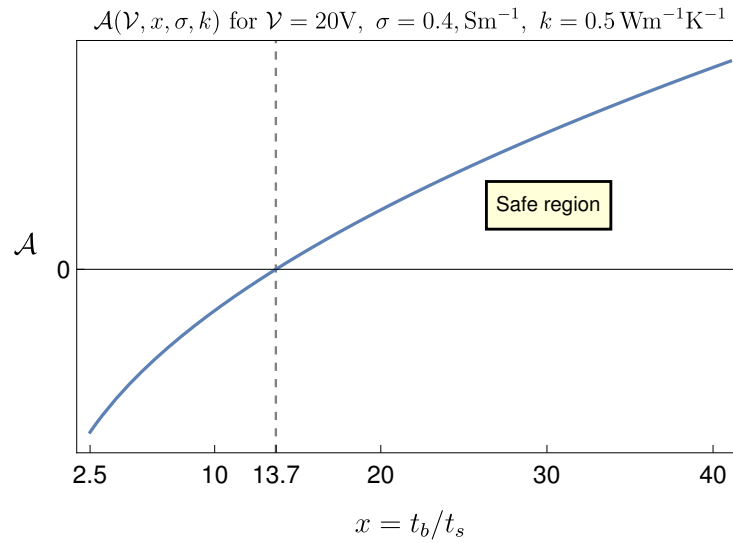


Figure 5. Critical choice of $x = t_b/t_s$ when $\mathcal{V} = 20\text{ V}$ (worst case) and $\sigma = 0.4\text{ Sm}^{-1}$, $k = 0.5\text{ Wm}^{-1}\text{ K}^{-1}$. Safety requires us to maintain $x > 13.7$.

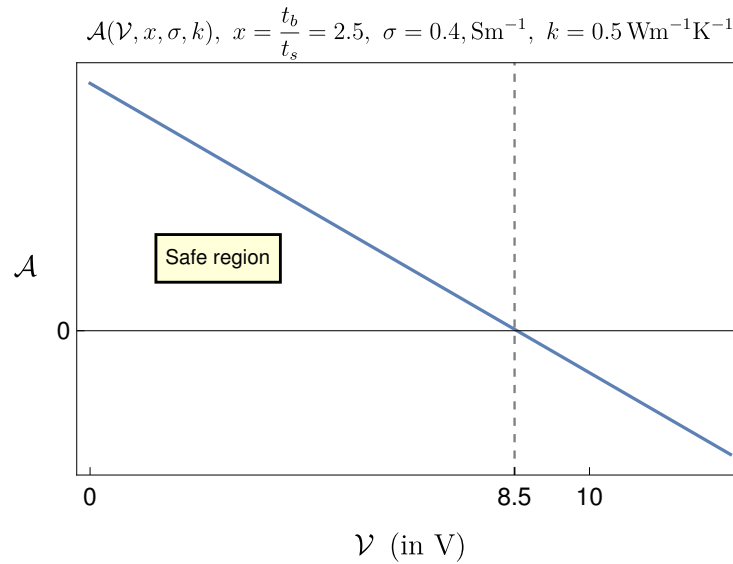


Figure 6. Critical voltage \mathcal{V} when $t_b/t_s = 2.5$ (worst case) and $\sigma = 0.4\text{ Sm}^{-1}$, $k = 0.5\text{ Wm}^{-1}\text{ K}^{-1}$. Safety requires us to maintain $\mathcal{V} < 8.5\text{ V}$.

A much worse scenario is offered when the current flows in an acidic medium, like gastric juice. In [11], the value of the gastric juice electrical conductivity was measured vs. pH, and a typical value was found to be $\sigma = 2\text{ Sm}^{-1}$, i.e., five times larger than the one of saliva. Clearly, the safety condition is now more severe, namely $\mathcal{V}^2 t_s/t_b < 5.8\text{ V}^2$; thus, (15) modifies (still approximately) to

$$\mathcal{V} < 2.4\sqrt{x}\text{ V}. \tag{16}$$

Figures 7 and 8 refer to this case, showing that the range of admissible selectable parameters is severely reduced.

For instance, the lower limit for x corresponding to $\mathcal{V} = 20\text{ V}$ raises to 68.5, which almost nullifies the therapeutic effect on the patient. In correspondence to $x = 2.5$ the constraint on \mathcal{V} is $\mathcal{V} < 3.8\text{ V}$, which is, in most cases, ineffective, making the procedure practically impossible. To have an idea of how to proceed in this case, let us revert to Expression (11) of the critical temperature with $\sigma = 2\text{ Sm}^{-1}$, namely

$$\vartheta(1) \approx 0.51\mathcal{V}^2 \frac{t_s}{t_b} \quad (\text{K}).$$

With an effective value $\mathcal{V} = 10 \text{ V}$, and requiring a maximum value for $\vartheta(1)$ of, say, 3 K , the choice for the ratio t_b/t_s must be such that $t_b/t_s > 17$, which is reasonable. Thus, still in this unfavorable situation, there is a way to safely perform the procedure, but selecting the voltage and the time parameters with care. Taking the extreme values $\mathcal{V} = 20 \text{ V}$ and $x = 2.5$ would produce, in this case, a temperature increase greater than 80 K , which is unbearable.

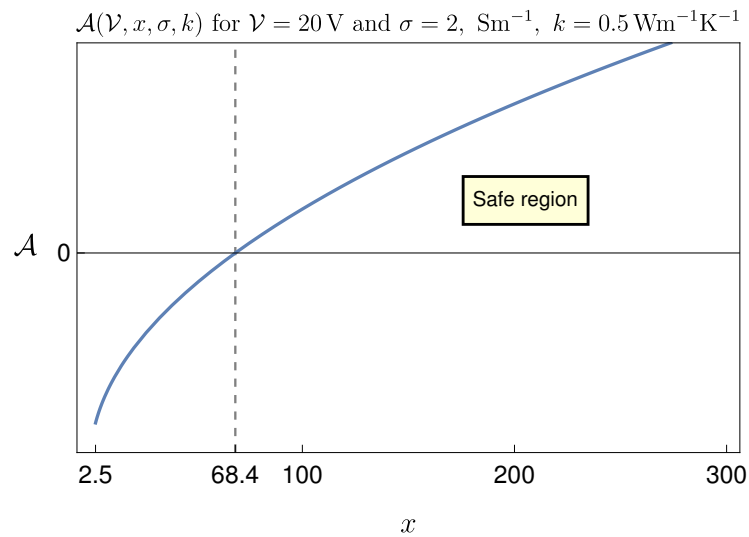


Figure 7. The safety operating time ratio $x = t_b/t_s$ for $\sigma = 2 \text{ Sm}^{-1}$ and $\mathcal{V} = 20 \text{ V}$ corresponds to $x > 68.5$.

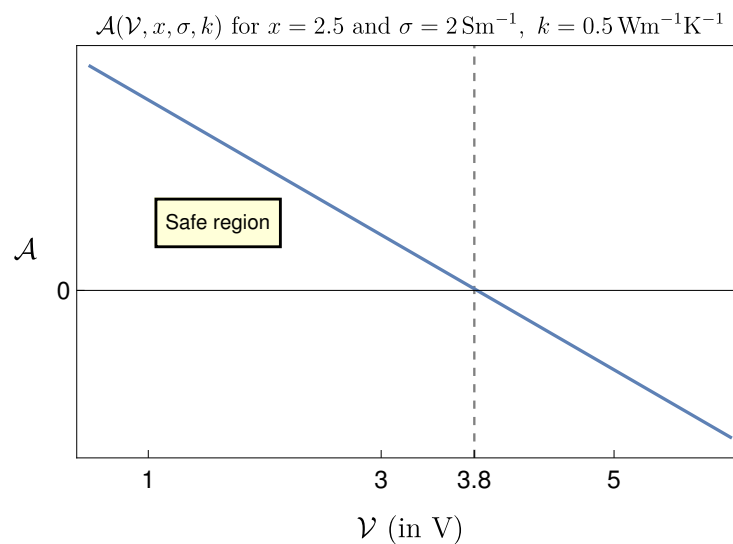


Figure 8. The safety operating voltage for $\sigma = 2 \text{ Sm}^{-1}$ and $x = 2.5$ corresponds to $\mathcal{V} < 3.8 \text{ V}$.

The conclusion is that the pulsed current stimulation of biological tissues is normally safe, but it may become critical in the presence of highly conductive (i.e., acidic) media. Stimulating at high voltage and with pulse duration close to the stimulation period requires that local pH value be previously checked and the ratio x suitably selected.

The safe operating condition $\mathcal{A}(\mathcal{V}, t_s, t_b; \sigma) > 0$ can be viewed in a three dimensional setting. The two panels in Figure 9 show, respectively, the region where $\mathcal{A} < 0$ (on the left) and three level sets of $\vartheta(1)$ (on the right) for $\sigma = 0.4$ when $\delta = 3 \text{ K}$. Figure 10 shows the same features when $\sigma = 2 \text{ Sm}^{-1}$.

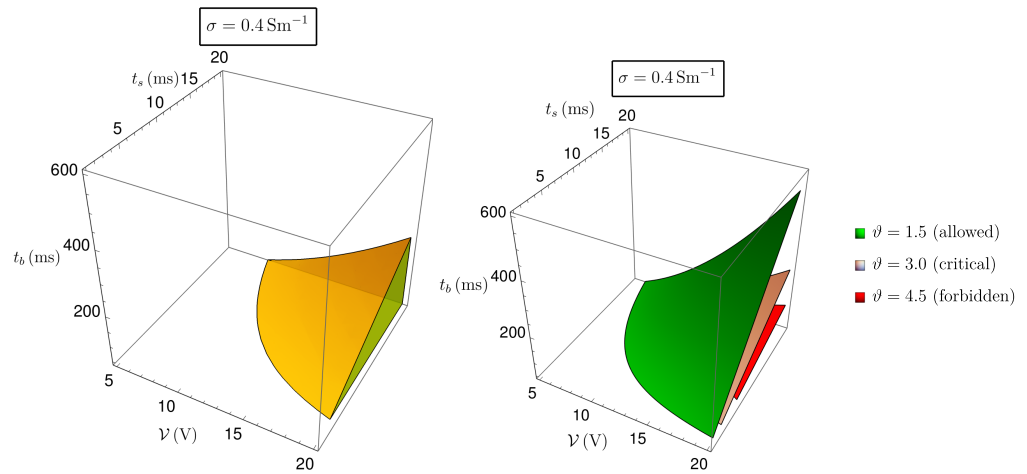


Figure 9. Three-dimensional representation of the forbidden region where \mathcal{A} is negative (on the right panel) and three level sets of $\vartheta(1)$ (on the left panel), when $\sigma = 0.4 \text{ Sm}^{-1}$.

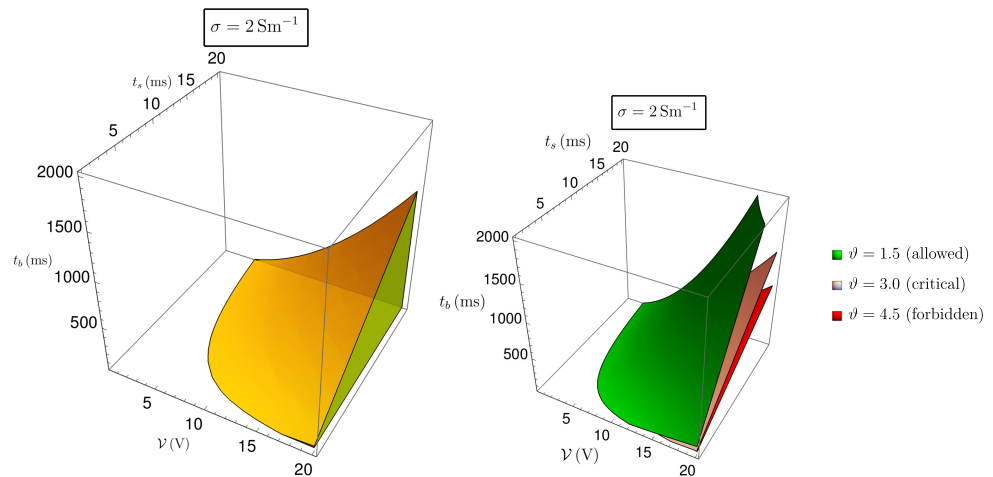


Figure 10. Three-dimensional representation of the forbidden region where \mathcal{A} is negative (on the right panel) and three level sets of $\vartheta(1)$ (on the left panel), when $\sigma = 2 \text{ Sm}^{-1}$.

4. Introducing the Effect of Blood Perfusion

Blood circulation has a stabilizing effect on temperature. In the specific case, it helps removing heat from the interested region. This feature can be introduced in the model by modifying the source term $P(r)$ in Equation (1) as follows: $P = P_0 = 3Q/(4\pi R^3)$ if $0 < r < R$ (unchanged) and $P = q_b c_b \omega (T - T_0)$ ($b = \text{blood}$), for $r > R$, representing the heat removing rate. Clearly, $q_b c_b \omega$ has dimension $\text{Wm}^{-3} \text{K}^{-1}$, and so ω has dimension s^{-1} . Indeed ω is the volume of blood crossing the unit volume of tissue in one second. For soft tissues, we can take $\omega \approx 3 \times 10^{-3} \text{ s}^{-1}$ or less (see [12–14]). Thus, the differential equation governing the temperature evolution is obviously the same, namely (1), but now (2) is replaced by

$$P(r) = \begin{cases} \frac{3Q}{4\pi R^3}, & \text{if } 0 < r < R, \\ q_b c_b R_e^2 \frac{\omega}{k}, & \text{if } R < r < R_e. \end{cases} \quad (17)$$

Proceeding as in Section 2, we first rescale r with R and t with t_{ref} , so to again formulate the problem in the steady state and in an unbounded domain. Finally, we introduce $u(r) = r\vartheta(r)$ so that the new system of differential equations to integrate is the following:

$$\begin{cases} \frac{u''}{r} = -G \mathcal{V}^2 \frac{\sigma t_s}{k t_b}, & 0 < r < 1 \\ u'' = \mu^2 u, & r > 1 \\ \lim_{r \rightarrow +\infty} \frac{u}{r} = 0, \quad u(0) = 0 \\ \llbracket u \rrbracket|_{r=1} = \llbracket u' \rrbracket|_{r=1} = 0. \end{cases} \quad (18)$$

Here, $\mu^2 = \rho_b c_b R^2 \omega / k$ (dimensionless). Recalling the estimate $R \approx 3$ mm, $k = 0.5 \text{ Wm}^{-1} \text{ K}^{-1}$, and that

$$\rho_b \approx 10^3 \text{ kg}^{-3}, \quad c_b \approx 3.6 \times 10^3 \text{ J kg}^{-1} \text{ K}^{-1},$$

we obtain $\mu \approx 0.44$. The solution to System (18) in terms of $\vartheta(r)$ is written as follows:

$$\vartheta(r, \mu) = \begin{cases} \frac{1}{6} \left(G \mathcal{V}^2 \frac{\sigma t_s}{k t_b} \right) \left(\frac{\mu + 3}{\mu + 1} - r^2 \right) & r \in (0, 1) \\ \frac{1}{3} \left(G \mathcal{V}^2 \frac{\sigma t_s}{k t_b} \right) \frac{\exp[\mu(1 - r)]}{r(\mu + 1)}, & r > 1. \end{cases} \quad (19)$$

Figure 11 shows that blood perfusion entails a significant reduction in the thermal fields given by (9). It is worth noting that if μ tends to zero, the no-perfusion solution is retrieved.

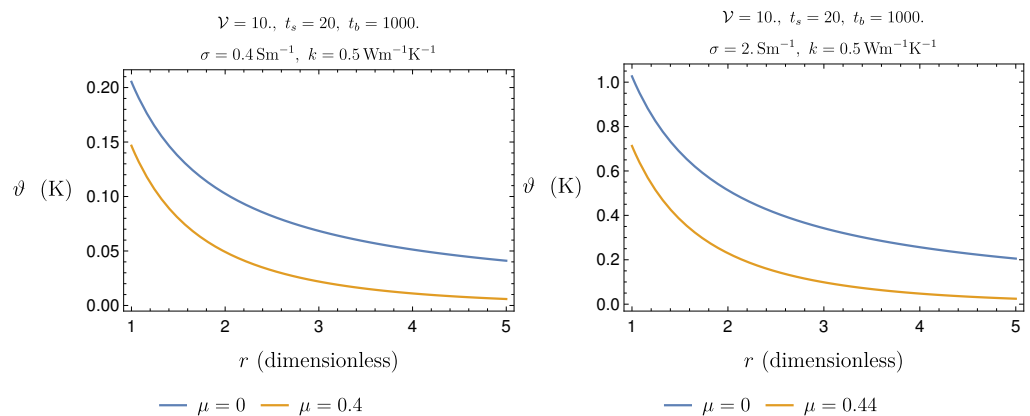


Figure 11. The effect of heat removal due to blood perfusion compared with the case in which perfusion is not taken into account.

Let us analyze the influence of perfusion on the safety conditions. From (19), we obtain

$$\vartheta(1, \mu) = \frac{G}{3} \left(\mathcal{V}^2 \frac{\sigma t_s}{k t_b} \right) \left(\frac{1}{\mu + 1} \right) \quad (20)$$

which clearly emphasizes the influence of perfusion; the corresponding relative change as a function of r is

$$\mathfrak{R}(r) = \frac{\vartheta(r, 0) - \vartheta(r, \mu)}{\vartheta(r, 0)},$$

hence, $\mathfrak{R}(1) = 0.3$ (see Figure 12).

Accordingly, the safety condition (14) changes as follows:

$$\frac{G \sigma}{3 k} \mathcal{V}^2 \frac{t_s}{t_b} \frac{1}{\mu + 1} < \delta, \quad (21)$$

which, for $\delta = 3 \text{ K}$, $\sigma = 0.4 \text{ Sm}^{-1}$, $k = 0.5 \text{ Wm}^{-1} \text{ K}^{-1}$, and $\mu = 0.44$ entails

$$\mathcal{V} < 6.46 \sqrt{x} V,$$

showing some improvement with respect to the no-perfusion case. For instance, for $\mathcal{V} = 20 \text{ V}$, this implies $x > 9.6$, allowing us to, e.g., increase t_s to 104 ms when $t_b = 1 \text{ s}$. Similarly, for $\sigma = 2 \text{ Sm}^{-1}$, we require

$$\mathcal{V} < 2.94\sqrt{x}\text{V},$$

with a certain improvement with respect to the corresponding condition (15).

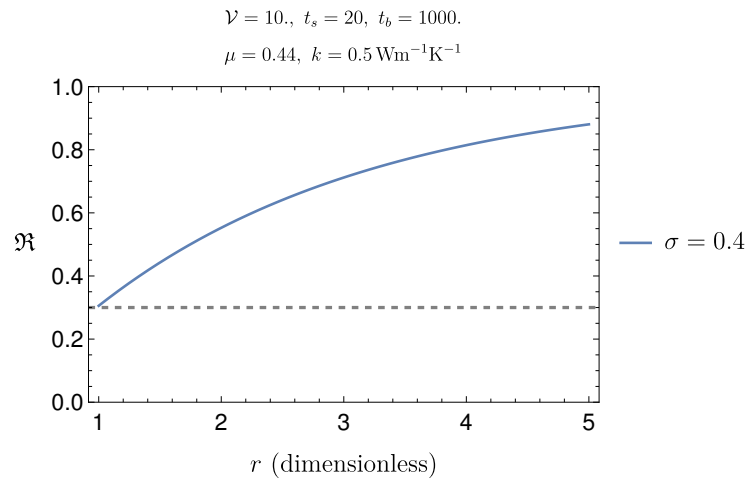


Figure 12. Function $\mathfrak{R}(r)$ shows the efficiency of perfusion in the area of interest.

In addition to safety conditions, it is reasonable to add some efficiency condition, because if \mathcal{V} is too small or x is too large, the treatment may not be effective. Thus, we impose the constraints $\mathcal{V} > \mathcal{V}_{\text{inf}}$ and $x < x_{\text{sup}}$ (for instance, $\mathcal{V}_{\text{inf}} = 8 \text{ V}$, $x_{\text{sup}} = 200$) and possibly also the lower limit $t_s > 20 \text{ ms}$. In view of these requirements, the suggestible parameters range are further reduced. Figure 13 shows the no-efficiency region when the above conditions are imposed for the respective cases $\sigma = 0.4 \text{ Sm}^{-1}$, $\sigma = 2 \text{ Sm}^{-1}$.

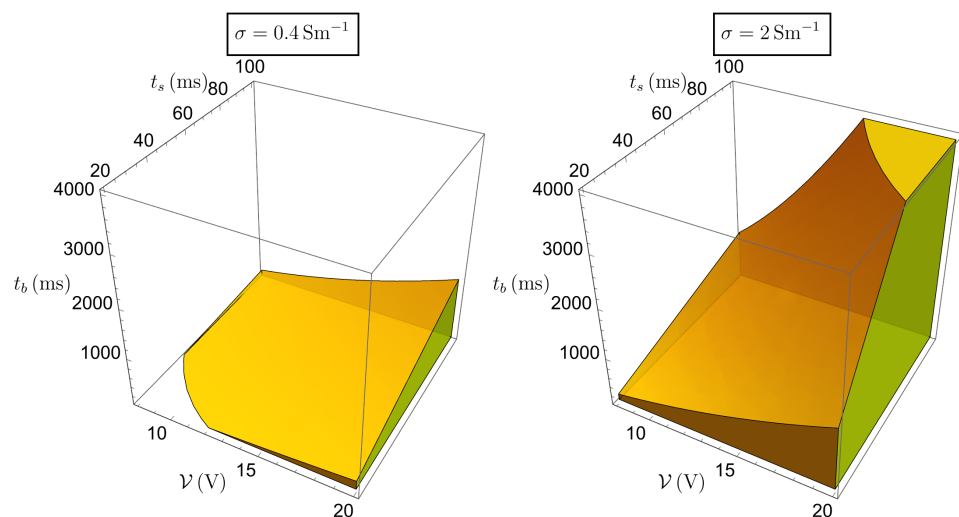


Figure 13. Three-dimensional representation of the region of settable parameters which, although larger than the unsafe one shown in the left panels of Figures 9 and 10 (and so containing safe values of the parameters), are not efficient from the therapeutic point of view. On the left side, case $\sigma = 0.4 \text{ Sm}^{-1}$; on the right side, case $\sigma = 2 \text{ Sm}^{-1}$.

5. Conclusions

The present contribution is motivated by a report by Köhler [3], concerning the risk of the esophagus wall during prolonged transesophageal pacing. In particular, the clinical

adverse event reported in [3] may be possibly caused by gastric reflux. We have formulated a mathematical model to predict the temperature increase caused by the application of a pulsating current in a body compartment, supplied in situ by a bipolar device. This issue is important in view of the fact that cells can die when exposed to temperatures of 41–42 °C for a long time. The main finding is that local acidity is a crucial quantity. Lowering pH (e.g., for a gastric reflux) may raise electrical conductivity to such a point as to make the treatment dangerous if the stimulating parameters are not selected with care. We computed the safety ranges for amplitude, duration, and period of the voltage pulses in correspondence to normal pH and to low pH, based on the data provided by the literature.

Author Contributions: A.F. (Angiolo Farina), A.F. (Antonio Fasano) and F.R. performed the formal analysis; the investigation; the validation procedure and the writing—review process. A.F. (Antonio Fasano) developed the conceptual model. F.R. developed the software. All authors have read and agreed to the published version of the manuscript.

Funding: This research received no external funding.

Data Availability Statement: Data are contained within the article.

Conflicts of Interest: The authors declare that they have no competing interests or other interests that might be perceived to influence the results and/or discussion reported in this paper.

References

1. Furman, S. Fundamentals of cardiac pacing. *Am. Heart J.* **1967**, *73*, 261–277. [[CrossRef](#)] [[PubMed](#)]
2. Nomura, R.; Shiraga, K.; Inuzuka, R. Successful transesophageal pacing in a very-low-birth-weight-infant with atrioventricular block. *Cardiol. Young* **2023**, *33*, 318–320. [[CrossRef](#)] [[PubMed](#)]
3. Köhler, H.; Zink, S.; Scharf, J.; Koch, A. Severe esophageal burn after transesophageal pacing. *Endoscopy* **2007**, *39*, E300. [[CrossRef](#)]
4. Tzeis, S.; Gerstenfeld, E.P.; Kalman, J.; Saad, E.B.; Sepehri Shamloo, A.; Andrade, J.G.; Barbhuiya, C.R.; Baykaner, T.; Boveda, S.; Calkins, H.; et al. 2024 European Heart Rhythm Association/Heart Rhythm Society/Asia Pacific Heart Rhythm Society/Latin American Heart Rhythm Society expert consensus statement on catheter and surgical ablation of atrial fibrillation. *Europace* **2024**, *26*, euae043. [[CrossRef](#)] [[PubMed](#)]
5. Pearce, J.A. Comparative analysis of mathematical models of cell death and thermal damage processes. *Int. J. Hyperth.* **2013**, *29*, 262–280. [[CrossRef](#)] [[PubMed](#)]
6. Fasano, A.; Sequeira, A. *Hemomath: The Mathematics of Blood*; MS&A; Springer: Cham, Switzerland, 2017; Volume 18.
7. Rattka, M.; Mavrikakis, E.; Vlachopoulou, D.; Rudolph, I.; Kohn, C.; Bohnen, J.; Yahsaly, L.; Siebermair, J.; Wakili, R.; Jungen, C.; et al. Pulsed field ablation and cryoballoon ablation for pulmonary vein isolation: Insights on efficacy, safety and cardiac function. *J. Interv. Card. Electrophysiol.* **2024**, *67*, 1191–1198. [[CrossRef](#)] [[PubMed](#)]
8. Cannon, J.R. *The One-Dimensional Heat Equation*; Encyclopedia of Mathematics and its Applications; Cambridge University Press: Cambridge, UK, 1984.
9. Fish, R.M.; Geddes, L.A. Conduction of electrical current to and through the human body: A review. *Eplasty* **2009**, *9*, e44. [[PubMed](#)]
10. Bianchi, L.; Cavarzan, F.; Ciampitti, L.; Cremonesi, M.; Grilli, F.; Saccomandi, P. Thermophysical and mechanical properties of biological tissues as a function of temperature: A systematic literature review. *Int. J. Hyperth.* **2022**, *39*, 297–340. [[CrossRef](#)] [[PubMed](#)]
11. Watson, S.J.; Smallwood, R.H.; Brown, B.H.; Cherian, P.; Bardhan, K.D. Determination of the relationship between the pH and conductivity of gastric juice. *Physiol. Meas.* **1996**, *17*, 21. [[CrossRef](#)] [[PubMed](#)]
12. Holmes, K.R. Thermal conductivities of selected tissues. In *Biotransport: Heat and Mass Transfer in Selected Tissues*; Diller, K.R., Ed.; New York Academy of Sciences: New York, NY, USA, 1998; pp. 18–19.
13. Ricketts, P.L.; Mudaliar, A.V.; Ellis, B.E.; Pullins, C.A.; Meyers, L.A.; Lanz, O.I.; Scott, E.P.; Diller, T.E. Non-invasive blood perfusion measurements using a combined temperature and heat flux surface probe. *Int. J. Heat Mass Transf.* **2008**, *51*, 5740–5748. [[CrossRef](#)] [[PubMed](#)]
14. Sharp, P. The measurement of blood flow in humans using radioactive tracers. *Physiol. Meas.* **1994**, *15*, 339. [[CrossRef](#)] [[PubMed](#)]

Disclaimer/Publisher’s Note: The statements, opinions and data contained in all publications are solely those of the individual author(s) and contributor(s) and not of MDPI and/or the editor(s). MDPI and/or the editor(s) disclaim responsibility for any injury to people or property resulting from any ideas, methods, instructions or products referred to in the content.